Dynamics of surfacealigned photochemistry (theory). II. Localized Hatom scattering in the HBr(ad)/LiF(001)+hv system

V. J. Barclay, D. B. Jack, J. C. Polanyi, and Y. Zeiri

Citation: The Journal of Chemical Physics **97**, 9458 (1992); doi: 10.1063/1.463967
View online: http://dx.doi.org/10.1063/1.463967
View Table of Contents: http://scitation.aip.org/content/aip/journal/jcp/97/12?ver=pdfcov
Published by the AIP Publishing

Dynamics of surface-aligned photochemistry (theory). II. Localized H-atom scattering in the HBr(ad)/LiF(001)+$h\nu$ system

V. J. Barclay, D. B. Jack,[a] J. C. Polanyi, and Y. Zeiri[b]
Department of Chemistry, University of Toronto, Toronto M5S 1A1, Canada

(Received 25 June 1992; accepted 8 September 1992)

The angular and energy distributions of 1.1 and 2.6 eV H-atom scattering from a LiF(001) surface are compared for two different sources of hot H-atoms (1) localized H-atoms produced by the photolysis of HBr molecules adsorbed on the LiF surface; and (2) H-atoms from a beam at the same energy and angle of approach to the LiF surface as in (1). These distributions are the results of classical stochastic trajectories carried out on a 7×7 slab of LiF(001). The calculated angular distributions are compared with experimental distributions [E. B. D. Bourdon *et al.*, J. Chem. Phys. **95**, 1361 (1991)]. The computed effects of changing H-atom energy and surface temperature are also reported; localized scattering becomes increasingly nonspecular at lower photon energies, and broader at higher surface temperatures.

I. INTRODUCTION

One of the aims of surface-aligned photochemistry is to control the outcome of a photo-induced reaction through the selection of reagent initial conditions.[1,2] In a favorable case this can be achieved by coadsorbing the reagents on a solid substrate, such as an ionic crystal, prior to the initiation of photodissociation (PDIS) and subsequent photoreaction (PRXN).[2] The adsorbed molecules will be aligned with respect to each other, oriented with respect to the surface, and positioned at localized adsorption sites. Subsequent photolysis of an adsorbed molecule can yield photofragments moving in preferred directions with respect to the surface and to neighboring adsorbate molecules.

Although the alignment of the adsorbate molecules provides the main constraint on the types of reactive events possible, the orientation of the adsorbate can also have a strong influence on the reaction outcome. If a photofragment is directed downward, adsorbate orientation requires that during or shortly after PDIS the fragment scatter off of the substrate surface before encountering a neighboring adsorbate molecule. This intermediate step alters but does not eliminate the preferred geometries in inelastic encounters with the coadsorbate. In such a case it is necessary to understand the dynamics of PDIS in the presence of the solid surface, as well as the subsequent photofragment plus surface scattering, before proceeding to study inelastic and reaction dynamics in photofragment plus adsorbate encounters.

Besides being a necessary preliminary to understanding the initial stages of adsorbate–adsorbate interactions in surface-aligned photochemistry, PDIS studies also yield information of a unique sort in regard to adsorbate–surface interaction. Experimentally this information is obtained through an examination of the angle and energy distributions of the scattered photofragments. Some such studies, experimental and theoretical, have been undertaken.[2]

The first to yield clear-cut evidence of surface scattering was the observation of atomic Br recoiling from CH_3Br on LiF(001) with a translational energy up to 0.6 eV in excess of the theoretical limit for Br recoiling from CH_3 in the gas-phase.[1,3] This was interpreted as being due to "chattering" of the light CH_3 between the heavy departing Br and the rigid surface; each to and fro motion of the CH_3 would impart additional momentum to the Br. Recently, Guo and Schatz[4] as well as Watson *et al.*[5] have modeled this process for the ICl/MgO(001) and CH_3Br/LiF(001) systems, respectively. Previously, McCarthy and Gerber,[6] in their theoretical work on the ICl/MgO(001) system, pointed out that photofragment scattering constitutes a promising tool for probing local surface properties. The same observation has been made in the work of this laboratory.[2,7,8] By virtue of the localized position of the adsorbate, surface-aligned photochemistry adds a new feature to surface scattering, namely selectivity in the site that is being struck. Site-selectivity makes this a more specific probe of the surface than is atomic or molecular beam scattering in which all points of the surface are equally sampled.

Adsorbate photolysis of HBr/LiF(001) has shown clear evidence of the involvement of surface-scattering.[7] Fast H-atoms were observed to be leaving the crystal surface with an angular distribution peaked at 55° from the surface normal. This observation is amenable to explanation in terms of localized-scattering since the alignment and orientation of the adsorbate has been established by polarized infrared absorption spectroscopy with implications for the positioning of the HBr, H being shown to be hydrogen-bonded to substrate F^-.[8] These observations have been confirmed in an independent theoretical study of the HBr/LiF(001) interaction.[9] There is therefore good reason to believe that for a HBr molecule in its equilibrium position the Br-atom sits above a Li^+ with the H-atom oriented downwards at $21°\pm5°$ with respect to the surface horizontal towards a neighboring F^-. The photolysis of a

[a]Dept. of Chemistry and Biochemistry, Concordia University, 1455 de Maisonneuve Blvd. W., Montreal, P.Q., H3G 1M8, Canada.
[b]Permanent address: Nuclear Research Center, Negev, Beer-Sheva, Israel 84190.

 0021-9606/92/249458-10$06.00

HBr molecule with this orientation yields a H-atom photofragment which scatters off a fluorine anion at a preferred impact parameter before desorbing from the surface or being subject to a reactive encounter with a neighboring HBr(ad) molecule.[2,7,9]

Adsorbate orientation and positioning prior to photolysis should therefore permit sampling of a local "target" region of the surface. Alteration of the photolytic wavelength will then allow the potential-energy contours at the sampling point to be mapped.[2]

In this paper, the second in a series of theoretical studies of the dynamics of surface-aligned photochemistry,[10] we report on a molecular dynamics study of the 193 and 248 nm PDIS of HBr adsorbed on the LiF(001) surface, and the subsequent scattering of the hot H-atom photofragments, with energies of 2.6 and 1.1 eV, respectively, off the LiF surface. This localized scattering of H-atoms is compared with scattering of an atomic beam of 2.6 eV H-atoms impinging upon the surface with the same polar and azimuthal angles as the preferred molecular axis of the adsorbed species. Stochastic trajectory methods are used to generate incident angle distributions of the H-atoms. The effects of temperature, photolysis energy, and increasing coverage on the incident and scattering angle distributions for localized scattering are also examined.

The adsorbate and photofragment motions at the surface are described by classical mechanics and are followed using a stochastic trajectory approach. These equations employ a "ghost particle" representation[11] to describe in an approximate manner the thermal motion of the solid surface. We consider only the nonreactive scattering dynamics; the study of reactions between the atomic photofragments and other adsorbed HBr molecules is the subject of a future paper.[12] A quantum mechanical treatment of the PDIS of HBr/LiF(001) using time-dependent wave packet methods[13] [similar calculations have been done for the ICl/MgO(001) system[4]] has been completed and will also be reported separately.[14]

II. METHOD OF CALCULATION

In order to model the photodissociation of HBr adsorbed on LiF(001) and the subsequent scattering of the H-atom photofragment it is necessary to have potential-energy functions which describe the repulsive interaction in the H·Br electronically excited state, as well as the interaction potential of the HBr molecule and H-atom with the LiF surface. It is then possible to run a molecular dynamics (MD) simulation. This simulation is separated into two phases. During the first phase a HBr molecule is placed near its equilibrium position above the LiF(001) surface, and then allowed to thermalize with the surface. When thermalization is complete the HBr molecule is "photolyzed" by changing the interaction potentials (within the molecule as well as with the surface) to those appropriate to the excited repulsive state. These potentials are then used in the second phase of the simulation to determine the motion of the photofragments during PDIS and surface scattering.

In this section we describe the methods and parameters used to construct the HBr/LiF adsorbate–surface interaction potential and the H·Br intramolecular potential. Since the charge distribution around a H-atom depends on whether it is a free atom or is bound to a Br atom, a distinction is made between the atomic and molecular states of the H-atom when assigning parameters for its interaction with the LiF surface. In principle the same is true for the Br-atom, but since the change is expected to be small and the Br moves very little during the course of the scattering event, no distinction between the molecular and atomic states of Br is made. We also outline the MD methods used to simulate the PDIS and scattering processes.

A. Potential functions

1. Interaction with the surface

The form of the potential functions used in this work were identical to those used previously in a study[9] of the structure of the HBr/LiF(001) system. The methods for calculating the parameters which characterize the gas–solid interaction have been refined as compared with those used for the calculation of the static structure. This has led to a change in some of the parameters to values better suited to a description of the dynamics of PDIS and surface scattering. These calculational methods, as well as the form of the potential functions, are outlined below.

The interaction between the LiF crystal and an adsorbed HBr molecule is considered to be the sum of classical electrostatic interactions, plus contributions arising from "core" interactions. To first order the electrostatic interaction may be described by a pair of point dipoles, fixed on the H and Br sites, immersed in the permanent electric field found at the surface of the LiF ionic crystal. For the (001) face of a face-centered-cubic (fcc) ionic crystal the electric field

$$\mathbf{E}(\mathbf{r}) = -\nabla\Phi(\mathbf{r}) \tag{1}$$

may be obtained from the electrostatic potential[15]

$$\Phi(\mathbf{r}) = \frac{4e}{a}\left[\frac{\exp\left(-\frac{2\pi z}{a}\right)}{1+\exp(-\sqrt{2}\pi)}\right]\left[\cos\left(\frac{2\pi x}{a}\right)+\cos\left(\frac{2\pi y}{a}\right)\right], \tag{2}$$

where a is the lattice constant of the crystal and e is the magnitude of the electronic charge on an individual ion. The coordinate system of the position vector $\mathbf{r}=(x,y,z)$ has its origin centered on the site of a surface Li^+ with the z axis perpendicular to the surface plane and the x and y axes in the surface plane pointing toward neighboring Li^+ sites (the [1,1,0] and [1,−1,0] directions of the standard crystal orientation). As in earlier work,[9] the dipole moments $\mathbf{p}_i = \mu_i\mathbf{u}$ were positioned along the unit vector $\mathbf{u}=(\mathbf{r}_1-\mathbf{r}_2)/|\mathbf{r}_1-\mathbf{r}_2|$, which pointed along the HBr molecular axis from the Br-atom at $\mathbf{r}_2$ to the H-atom at $\mathbf{r}_1$, with values of $\mu_1=1.4146$ D at the hydrogen site and $\mu_2=-0.5866$ D at the bromine site. These orientations and values for the point dipoles reproduce the experimental values for the

TABLE I. Calculated Tang–Toennies gas–atom plus surface–ion potential parameters.

Interaction	A (keV)	β (Å^{-1})	C_6 (eV Å^6)	C_8 (eV Å^8)
H(atom)–Li$^+$	0.175	3.78	0.125	0.196
H(atom)–F$^-$	0.174	2.88	2.585	3.404
H(mol)–Li$^+$	0.189	4.50	0.125	0.196
H(mol)–F$^-$	0.177	3.28	2.585	3.404
Br(mol)–Li$^+$	2.370	4.63	1.637	2.568
Br(mol)–F$^-$	0.727	3.35	37.14	48.94

dipole and quadrupole moments and give a reasonable value for the octupole moment.

Although it would have been computationally advantageous to use a two point charge model, such a model cannot reproduce the quadrupole and higher order moments and hence does not yield an adsorbate orientation consistent with the infrared (IR) experimental results.[8] Instead, the two point-dipole model described above is used so that the electrostatic interaction energy of a single HBr molecule above the LiF(001) surface is written as

$$V(\mathbf{r}_1,\mathbf{r}_2)=\sum_{i=1}^{2}\mathbf{p}_i\cdot\mathbf{E}(\mathbf{r}_i)=\sum_{i=1}^{2}\mu_i\mathbf{u}\cdot\mathbf{E}(\mathbf{r}_i). \tag{3}$$

The "core" interactions, comprised of repulsion (Pauli exclusion) and dispersion (van der Waals) interactions, between the LiF crystal and an adsorbed HBr molecule are quantum mechanical in origin. They are treated as being pairwise additive. The assumption of pairwise additivity allows the potential to be written in terms of two body interactions between each constituent atom of the admolecule and the individual ions of the substrate. The total potential due to the "core" interactions is obtained by summing over all distinct pairs of adsorbate and substrate sites.

For two atoms (one of adsorbate, one of substrate) separated by a distance r the "core" interaction potential is assumed to be described by the Tang–Toennies potential,[16]

$$V(r)=A\exp(-\beta r)-\sum_{n=3}^{\infty}\left[f_{2n}(r)\frac{C_{2n}}{r^{2n}}\right], \tag{4}$$

where

$$f_{2n}(r)=1-\sum_{k=0}^{2n}\left[\frac{(\beta r)^k}{k!}\right]\exp(-\beta r) \tag{5}$$

is a phenomenological damping function. The C_{2n} coefficients define the dispersion series of which only the first two terms were retained. The values of the C_6 and C_8 coefficients (listed in Table I) were taken to be the same as those used in our earlier study.[9] By contrast the Born–Mayer parameters, A and β, are not the same as those used previously.

Typically, the short-range repulsive potential between two atoms, i and j, is approximated by the Born–Mayer potential,

$$V_{ij}(r)=A_{ij}\exp(-\beta_{ij}r), \tag{6}$$

where the parameters A and β characterize the strength and range, respectively, of the potential. The previous estimate of the Born–Mayer parameters, based on known atom–atom and bulk crystalline ion–ion data, made use of the simple geometric mean combining rule which works best for atomic species of a similar size. Due to the size discrepancy between the interacting adsorbate atoms and substrate ions a more sophisticated set of combining rules, detailed below, was used in the present work. Furthermore, surface ion–ion data has been used instead of the bulk properties, and a distinction has been made between hydrogen in the molecular and atomic states.

Though rarely known for unlike atoms, the Born–Mayer parameters can be constructed from sets of parameters for like atoms using combining rules. The simplest such rules use the geometric mean of the like–atom interactions. However, to account for difference in size between two interacting atoms Gilbert[17] and Smith[18] proposed the following rules for combining Born–Mayer parameters:

$$A_{ij}=\left[\frac{(\beta_{ii}+\beta_{jj})}{2\beta_{ii}\beta_{jj}}\right](A_{ii}\beta_{ii})^a(A_{jj}\beta_{jj})^b;$$
$$\beta_{ij}=\frac{2\beta_{ii}\beta_{jj}}{(B_{ii}+\beta_{jj})}, \tag{7}$$

where the exponents a and b are defined as

$$a=\beta_{jj}/(\beta_{ii}+\beta_{jj});$$
$$b=\beta_{ii}/(\beta_{ii}+\beta_{jj}). \tag{8}$$

These combining rules have been shown[19,20] to be more accurate than the geometric mean rules; accordingly they have been used here.

In order to use the above combining rules to construct the repulsive part of the Tang–Toennies potential for the various {H,Br}–{Li$^+$,F$^-$} interactions, it is necessary to have the four "like-pair" interactions. For the substrate ions it is necessary to make a distinction between the ions at the surface and those in the bulk of the solid since, as Fowler *et al.*[21,22] have shown, the electronic properties of an atom or ion can depend strongly on its local environment.

Accordingly, in estimating the Born–Mayer parameters for the Li$^+$–Li$^+$ and F$^-$–F$^-$ parameters we have made use of the parameters for the Li$^+$ and F$^-$ surface ions given by Fowler and Hutson[21,23] in their study of He scattering off of LiF and NaCl surfaces. When Gilbert and Smith's combining rules are applied to these data, along with the Tang and Toennies result[24] for He–He interaction, a set of Born–Mayer parameters for the Li$^+$–Li$^+$ and F$^-$–F$^-$ interactions can be extracted. Parameters for the H–H interactions were obtained from *ab initio* calculations; the molecular H parameters were obtained from work on the CH_3F–CH_3F interaction[25] while the atomic H parameters come directly from studies of the H_2 triplet state.[19,26] The Br–Br interaction was based[27] upon the parameters for the Kr–Kr interaction.[23] For simplicity these same parameters were used for Br in its atomic state.

Use of Gilbert and Smith's combining rules then yielded Born–Mayer parameters for the various adatom–substrate ion pairs, i.e., H–Li$^+$, Br–F$^-$, etc., needed for the

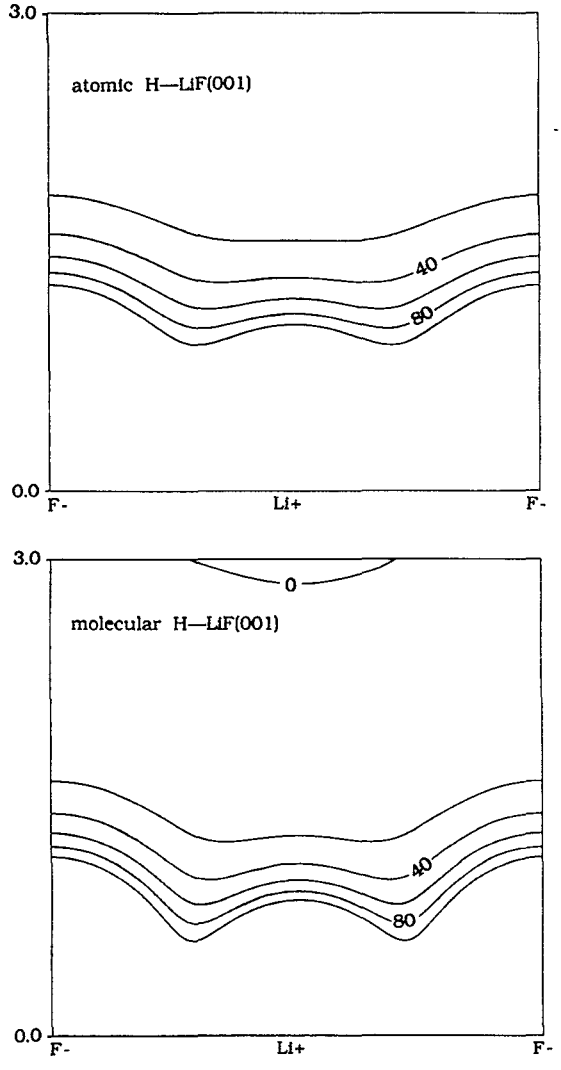

FIG. 1. (a) Interaction potential of atomic H with the LiF surface as a function of height z above the surface and distance x along the [100] crystallographic axis, using the parameters listed in Table I. The contours are in increments of 20 kcal/mol. (b) Interaction potential of molecular H (as in HBr) with the LiF surface. Coordinates and contour increments are as in (a).

Tang–Toennies potential [Eqs. (1)–(2)]. These parameters are listed in Table I along with the dispersion coefficients. The parameters used in the present work show a somewhat higher degree of surface corrugation than previously.[9] Figure 1 shows the surface corrugation for atomic hydrogen in comparison to hydrogen bound in a molecular state (corrugation is less marked for the diffuse atomic H). The range of interaction for atomic H is comparable to that obtained by Chow and Thompson[28] from data on the scattering of thermal (25 meV) H atoms off a LiF(001) surface.

As has been shown by Steele,[29] the pairwise summation of the adsorbate–substrate potential over the ionic lattice can be replaced by a two-dimensional Fourier series. This procedure has previously been applied to the HBr/LiF(001) system and the resulting form of the surface potential can be found in Ref. 9. The "core" contribution to the surface potential ultimately takes the form of a table of Fourier coefficients whose amplitudes are functions of the height z above the surface. As with the electrostatic interactions described above, this contribution is periodic in the lateral (x,y) plane.

This total adsorbate–surface potential, based on the new parameters, has been used in a Monte Carlo algorithm described previously,[9] in order to recalculate the equilibrium geometry of the HBr/LiF(001) system at 1.0 ML coverage. Qualitatively the structure was the same as before, though the HBr molecules moved in 6% closer to the Li^+ site (height z was 2.45 Å instead of 2.6 Å) and the polar angle decreased slightly from 23° to 20° below the surface horizontal plane. For a single molecule on the surface the polar angle was 26° below the surface horizontal as found previously.[9]

2. Interaction within HBr

In the gas-phase the excited repulsive states of H·Br are typically characterized by a set of curves, the appropriate curve being specific to the electronic state of the atomic products. Since these curves decay exponentially to their asymptotic values they can be reasonably approximated by a potential function of the Born–Mayer type. Of particular interest in this paper is the case when the H and Br photofragments separate into their neutral electronic ground states. For this state in the gas-phase the photolysis of HBr by 193 nm laser radiation yields a H-atom with a kinetic energy of 2.6 eV.

However, with the HBr molecule in direct contact with the LiF surface during PDIS such a simple description is no longer possible and differences between PDIS in the adsorbate and gas phases should be expected. We would expect the asymptotic kinetic energy of the H-atom photofragment originating from the adsorbed phase to be less than that in the gas phase ($E_{\mathrm{TRANS}} < 2.6$ eV) because of energy transfer to the solid during dissociation and the need to overcome the heat of adsorption.

Recent theoretical work on the PDIS of adsorbed molecules has shown differences between PDIS in the adsorbed and gas phases. In a report on the PDIS of CH_3Br/LiF(001) Watson *et al.*[5] showed a downward shift in the CH_3 photofragment kinetic energy distribution as compared to the gas phase. As expected the magnitude of this shift depended on the heat of adsorption.

In a study on the PDIS of IBr/MgO(001) McCarthy *et al.*[30] showed that there should be a pronounced difference between the gas-phase and surface PDIS line shapes. This difference reflects the changes in interaction with the surface as the bond length of the admolecule changes. These changes can be obtained from the unmodified gas-phase intramolecular potentials provided the adsorbate–surface interaction is included. To describe the bound state potential of the HBr molecule we used a Morse potential appropriate to the gas, with the values for the depth, range, and equilibrium distance parameters set at $D_e = 90.4$ kcal/mol, $\beta = 1.809$ Å^{-1}, and $r_e = 1.4138$ Å, respectively.

The repulsive state can be modeled by a Born–Mayer potential. We relax the requirement that the pre-

exponential factor maintain its gas-phase value and allow it to become a function of position and orientation, viz.,

$$V[\mathbf{r}_1(t),\mathbf{r}_2(t)]=A[\mathbf{r}_1(0),\mathbf{r}_2(0)]\exp[-b\cdot r(t)], \quad (9)$$

where $r(t)=|\mathbf{r}_1(t)-\mathbf{r}_2(t)|$, and the decay constant, calculated according to the combining rules given above, set at $b=3.50$ Å^{-1}. The pre-exponential factor $A[\mathbf{r}_1(0),\mathbf{r}_2(0)]$ is a function of the positions of the admolecule's constituent atoms at the time of photolysis ($t=0$); its method of calculation is described below.

According to this model the photon energy, $E(h\nu)$, is equal to the excitation energy, $E(\mathbf{r}_1,\mathbf{r}_2)$, of the HBr molecule to the repulsive state plus ΔE which includes the electrostatic contribution to the heat of adsorption of HBr(ad) and the repulsion between the H of the excited Br·H and the adjacent F^-,

$$E(h\nu)=E(\mathbf{r}_1,\mathbf{r}_2)+\Delta E.$$

The contributions to the "energy-shift" ΔE are

$$\Delta E=V_C^{\text{H-LiF}}(\mathbf{r}_1)+V_C^{\text{Br-LiF}}(\mathbf{r}_2)-V_C^{\text{HBr-LiF}}(\mathbf{r}_1,\mathbf{r}_2) - V_E^{\text{HBr-LiF}}(\mathbf{r}_1,\mathbf{r}_2), \quad (10)$$

where the first, second, and third terms V_C are the core interactions of the H atom, Br atom, and HBr molecule, respectively, with the LiF crystal, and the fourth term V_E is the HBr–LiF electrostatic interaction energy. The pre-exponential factor in Eq. (9) is calculated by requiring that the repulsive potential energy equal the photon energy minus the binding energy D_e of the H–Br molecule and the energy-shift ΔE, i.e.,

$$A(\mathbf{r}_1,\mathbf{r}_2)\exp(-br)=E(h\nu)-D_e-\Delta E. \quad (11)$$

B. Molecular dynamics

Classical trajectories were calculated by numerically integrating Hamilton's equations of motion using the interaction potentials given in Sec. II A. A stochastic element entered the calculation of the trajectories through the coupling of the adparticles to the vertical motion of the substrate.

During a photofragment–surface collision only a small portion of the "hot" H-photofragment kinetic energy is transferred to the substrate. Rather than calculate the motion of the substrate explicitly, the effects of recoil and thermal motion of the substrate ions on the trajectories of the adparticles were incorporated through the use of "ghost particles."[11] It should be noted that this only simulates the time-varying distortion of the surface along z. This technique assigned to each adatom a ghost (fictitious) particle moving along the substrate surface. The location of the ghost particle in the lateral direction (x and y) was fixed to be identical to that of the adparticle to which it was assigned. Coupling between the motion of the adparticles and their ghost particles occurs only for motion of the adparticle along the z direction, i.e., normal to the surface. The motion of the ghost particle in the z direction is described through an equation of motion of the Langevin type, viz.,

$$m_s(x,y)\ddot{s}=-\frac{\partial V_s(x,y,z,s)}{\partial s}-K(x,y)s - m_s(x,y)\eta\,\dot{s}+F(t), \quad (12)$$

where s is the deviation in the z direction of the ghost particle from its equilibrium position at the substrate surface, x, y, and z are the coordinates of the adparticle, and $V_s(x,y,z,s)$ is the normal adparticle–substrate surface potential. The quantity $F(t)$ is a Gaussian random force[11] whose strength G is related to the friction coefficient η, ghost particle mass $m_s(x,y)$, and substrate temperature T through the second fluctuation–dissipation theorem,

$$G=2\eta\,k_BTm_s(x,y). \quad (13)$$

By assuming the Debye model for the LiF substrate's phonon spectrum, the friction coefficient η and the force constant $K(x,y)$ may be approximated as[31]

$$\eta=\pi\omega_D/6,$$

and

$$K(x,y)=m_s(x,y)\omega_D^2/3, \quad (14)$$

respectively, where ω_D is the Debye frequency of the LiF crystal and $m_s(x,y)$ is the mass of the ghost particle. The ghost particle mass and its force constant are functions of the position of the ghost particle within the surface unit cell of the substrate. When the adparticle was above the Li^+ site the mass of the ghost particle was taken to be that of the lithium cation, and when it was above the F^- site its mass was that of the fluorine anion. The mass at all other positions was obtained using cosine interpolation. The frequency of oscillation of the fictitious particle was independent of its position in the surface unit cell.

Initially, the adsorbed HBr molecule was placed on the LiF(001) surface close to its equilibrium position (as ascertained in previous computations[9]), i.e., with the bromine atom over a Li^+ ion, and the hydrogen atom tilted down towards a F^- so that the bond axis formed an angle of 26° with the horizontal of the surface plane. The HBr molecule was then allowed to thermalize with the surface by integrating the equations of motion for ~1000–2000 time steps of 10 a.u. each (1 time a.u.≈0.025 fs). The adsorbed HBr molecule was considered to have thermalized with the surface when the average kinetic energy of the adsorbate was characterized by a temperature within 2% of that of the substrate. During this process the constituent adatoms were subject to random forces via their ghost particles, so that an ensemble of thermalized particles contained a distribution of admolecule orientations, positions and velocities.

Upon photolysis the H·Br interaction in the excited state was taken to be that of the Born–Mayer type as described by Eq. (9). Similarly the potential for the H–surface interaction was altered to reflect the creation of a H-atom photofragment. The Br–surface interaction was assumed to be unchanged. As in the case of molecular HBr, the ion-induced dipoles on both H and Br have been ignored since they contribute only ~5% to the atom–

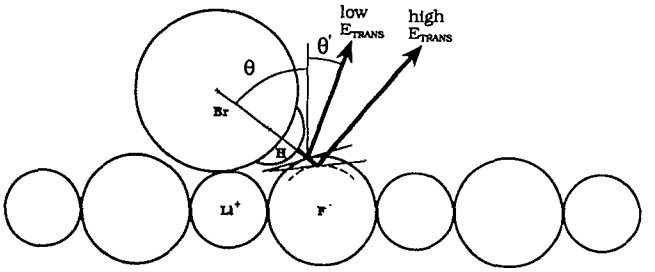

FIG. 2. Scattering geometry of a H-atom photofragment off a neighboring F^- ion at low and high collision energies, E_{TRANS}.

surface interaction energies for HBr at equilibrium separation directly following photolysis. The atom–surface interaction is dominated by repulsion and dispersion forces. The photofragment and ghost particle motions were then propagated (integrated in time step increments of 1 a.u.) until the scattered H-atom reached a height of $z=8$ Å above the surface. This required on average a total of 3000 time steps. The statistics for the angular distributions were obtained from a collection of 2000 trajectories.

In order to highlight the effect of orientation of the adsorbed HBr on the scattering angle of the H-atom photofragment a series of trajectories was run which simulated the scattering of a *beam* of H-atoms striking the LiF(001) surface. The H-atoms were placed at a height $z=8$ Å above the surface and directed downward with a kinetic energy of 2.6 eV at an angle of incidence of 64° with respect to the surface normal. The azimuthal angle was fixed at 45 ±0.05°. In order to simulate a beam with nonzero breadth the lateral coordinates (x,y) of the initial position of the H-atom were chosen randomly over the range $0 \leqslant x,y \leqslant a$, where $a=4.03$ Å is the lattice constant of LiF. The H+surface parameters for atomic H were used throughout the simulation. Trajectories were propagated in 1 a.u. time steps until the scattered H-atom reached a height of 8 Å above the surface. Approximately 2000 trajectories were run.

III. RESULTS AND DISCUSSION

A single HBr molecule adsorbed on the (001) surface of LiF rests with the Br-atom approximately over the top of a Li^+, with the H-atom pointing downwards toward a F^- at an angle of $\theta=26°$ below the surface horizontal. As illustrated in Fig. 2, photolysis of a HBr molecule with this orientation will direct a H-atom towards the surface with an angle of incidence of $\theta=64°$ relative to the surface normal (Fig. 2). The scattering angle θ' with which the H-atom recoils from the surface depends upon the local corrugation of the surface struck by the H-atom. For a perfectly flat surface we would have specular scattering, $\theta=\theta'=64°$. However, with the HBr molecule situated in its equilibrium position and orientation, the computation shows that the scattering angle is less than specular, i.e., $\theta'=55°$, indicating that the H-atom has struck the near side of a neighboring F^-; reflection is off a tangent to the F^- corrugation, tilted by 5° toward the surface normal.[2,7,9]

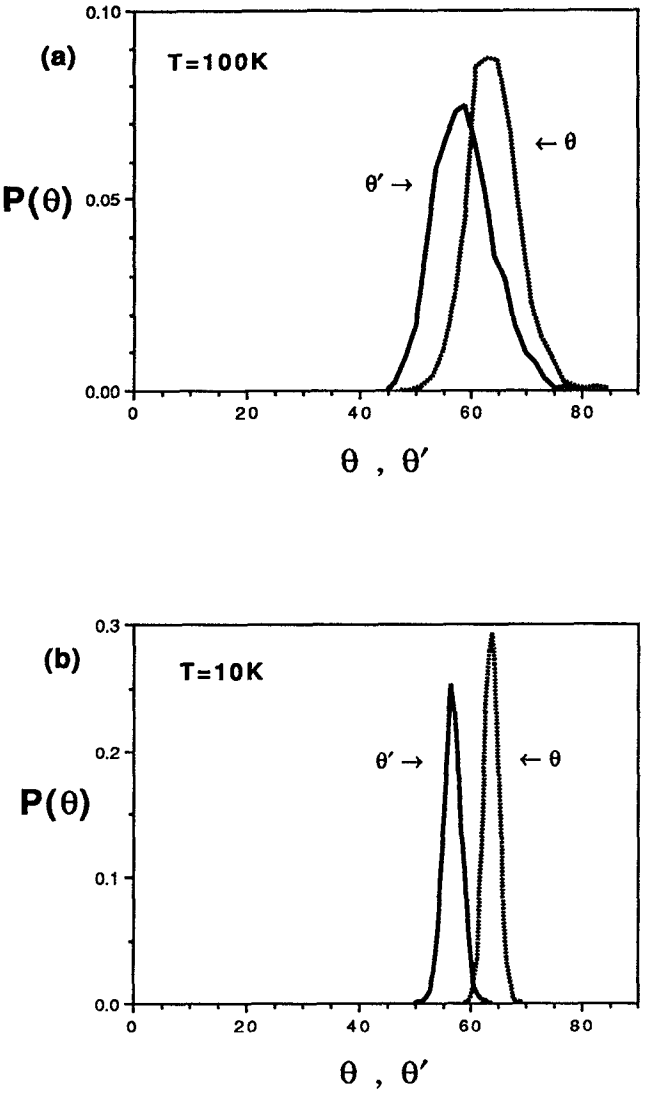

FIG. 3. (a) Distributions of the incident and scattering angles at 100 K (dashed and solid curves, respectively). The peak in the incident angle distribution occurs at $\theta=64°$ and the peak of the scattering angle distribution occurs at $\theta'=59°$. The FWHM are 11° and 13°, respectively. (b) Distributions of the incident and scattering angles at 10 K (dashed and solid curves, respectively). The peak in the incident angle distribution occurs at $\theta=64°$ and the peak of the scattering angle distribution occurs at $\theta'=56°$. The FWHM are 3° and 4°, respectively.

This tangent is shown schematically in Fig. 2, where the ionic radii for Li^+ and F^- were taken from Tosi[32] and the van der Waals radii for the Br and H atoms were obtained from the crystallographic data of Sandor and Johnson.[33] This less-than-specular scattering angle accords well with experiment.

We show the relevant findings in Fig. 3. The wavelength of the photolyzing radiation was assumed to be 193 nm so that the nominal energy (E_{TRANS}) of the H photofragments was 2.6 eV. The computed orientation of the HBr molecule has a thermal distribution about its equilibrium orientation that gives a distribution of values for the angle of incidence and hence the angle of reflection. These distributions are shown for temperatures $T=100$ and 10 K in Figs. 3(a) and 3(b), respectively. For both temperatures the full-width at half-maximum (FWHM) of the

scattered angle distribution is only marginally larger than the FWHM of the incident angle distribution. There is, however, a narrowing of the distributions as the temperature decreases from 100 to 10 K, the FWHM decreasing from 13° to 4°. There is also a shift of the peak to a larger angle at the higher temperature; at $T=10$ K, $\theta'=55°$, at $T=100$ K, $\theta'=60°$. A similar effect for the translational energy distribution of the scattered H-atom is reported below.

These features are favorable for the future studies of surface-aligned photoreaction since they show that the scattering of the H-atom photofragment off the surface in a single collision alters the direction of motion but does not entail significant loss of directionality. Should the H-atom enter into a reaction with a neighboring HBr(ad) molecule it would do so with a restricted angle of approach and impact parameter since it retains its memory of the aligned and oriented conditions of the initial state. The degree of alignment in the subsequent encounter can be varied through the substrate temperature. At low temperatures the scattering angle distribution of the H-photofragment is narrow, broadening at higher temperature [Fig. 4(a)]. With broadening of the distribution, reaction channels which were inaccessible at low substrate temperature may open up.

To further illustrate the constraints that the surface imposes on scattering originating in the adsorbed state, the above results have been compared with those for the scattering of a beam of H-atoms incident on the surface. The beam was directed towards the surface with the same energy (2.6 eV), angle of incidence ($\theta=64°$), and azimuthal angle as the adsorbed HBr but with a much smaller ($\pm 0.05°$) spread in the initial angular distributions. However, the impact points of the H-atoms were varied randomly since the beam will have a macroscopic width and will sample all parts of a unit cell at the surface. In so doing it will acquire a corresponding breadth in its scattering angle distribution.

As shown in Fig. 4, the H-beam yielded distributions which differed from those obtained from adsorbed state ("localized") scattering. The peak of the H-beam scattering angle distribution was at $\theta'=66°$ indicating that on average the beam scattered in a specular fashion. At a substrate temperature of 100 K the FWHM of this distribution was $\sim 10°$, slightly less than the adsorbed-state result of 13°. This similarity of the H-beam and adsorbed-state results is deceptive. The breadth in the adsorbed-state scattering angle is almost entirely due to the spread in the incident angle due to thermal motion of the adsorbate, whereas the H-beam was started out with a fixed incident angle (i.e., 0.1° width) and acquired a 10° width from scattering off all regions of the surface. For the H-beam this spread is intrinsic to the scattering process; lowering the substrate temperature will not narrow the scattering angle distribution appreciably. However, at low enough temperatures the spread of the adsorbed-state scattering becomes less than that for the H-beam since the surface region sampled is more precisely defined due to cooling of the adsorbate and hence a more precise position and orientation of the adsorbed HBr.

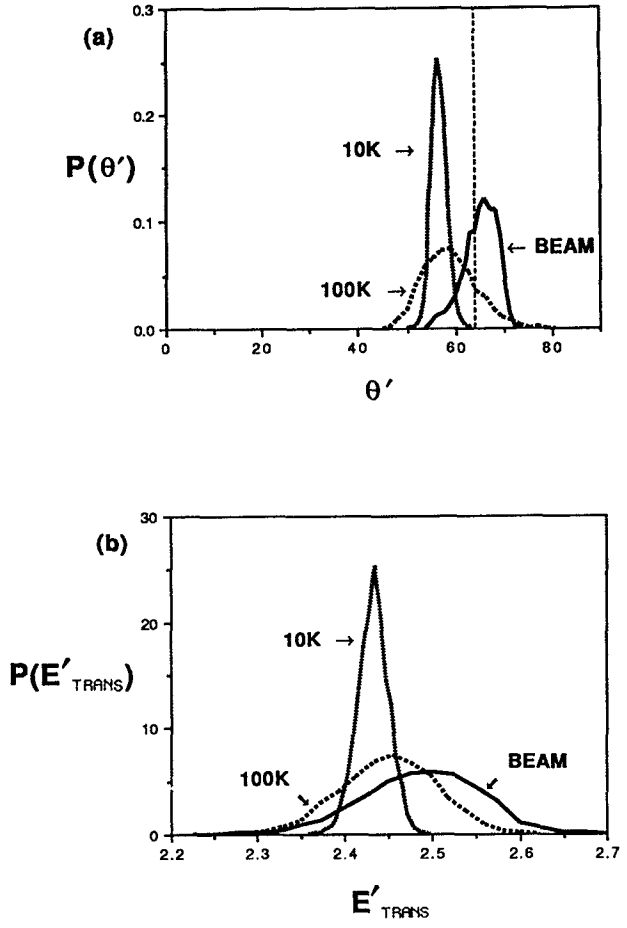

FIG. 4. (a) Comparison of the scattering angle distributions for H-atom photofragments originating from adsorbed HBr at 10 K (dotted curve) and 100 K (dashed curve), i.e., localized scattering, and from an H beam at 100 K (solid curve). The peak of the scattering angle distribution for the H-beam occurs at $\theta'=66°$ and the value of its FWHM is 10°. A vertical dashed line indicates the specular scattering angle. (b) Comparison of the translational energy distributions of scattered H-atom photofragments originating from adsorbed HBr at 10 K (dotted curve) and 100 K (dashed curve), i.e., localized scattering, and from a H beam at 100 K (solid curve). The peak of the scattering angle distribution for the H-beam occurs at $\theta'=66°$ and the value of its FWHM is 10°.

Similarly, Fig. 4(b) shows differences between the H-beam and adsorbed state distributions for the translational energy, E'_{TRANS}, of the scattered H-atoms. The peak of the H-beam translational energy was at 2.5 eV showing that the scattered H-atoms have lost 0.1 eV of energy to the surface. The scattered H-atoms originating from the adsorbed state lost more energy to the surface and showed a decrease of ~ 0.15 eV from the gas-phase value of 2.6 eV. The difference in the positions of the H-beam and adsorbed state peaks was due to the H-atom's contribution to the heat of adsorption of the HBr molecule in the adsorbed state and hence lower initial translational energy of the H. At a substrate temperature of 100 K the FWHM (0.12 eV) of the adsorbed state distribution was smaller than the FWHM (0.16 eV) of the H-beam distribution. The adsorbed state distribution sharpened further to a FWHM of

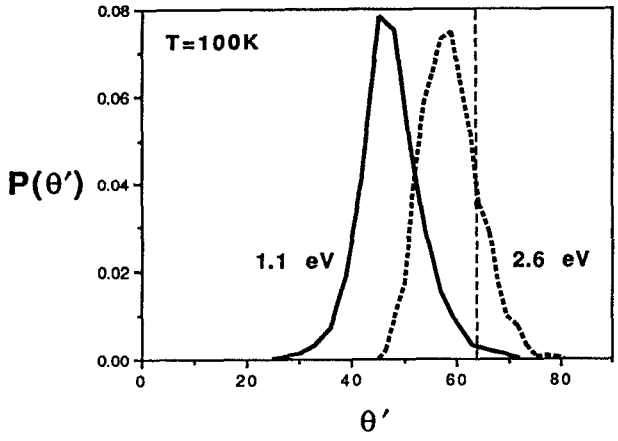

FIG. 5. Comparison of the computed angular distributions θ' for H photofragments produced by 193 nm (dashed curve) and 248 nm (solid curve) radiation with a substrate temperature of 100 K. The peak of the scattering angle distribution for the 248 nm radiation is calculated to occur at $\theta'=45°$ with a FWHM of 11°. The vertical dashed line indicates the specular value of θ'.

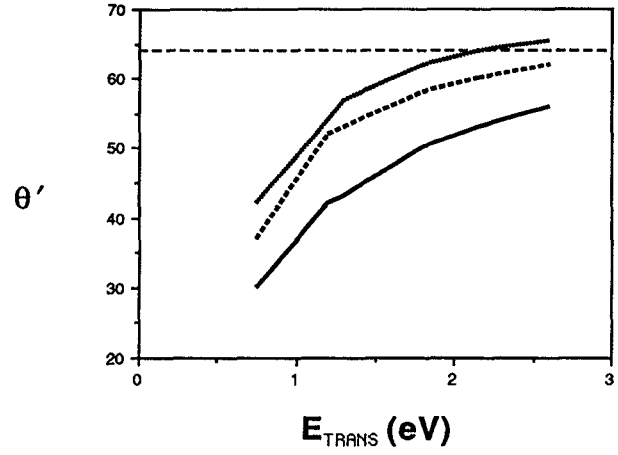

FIG. 6. Scattering angle as a function of H-atom kinetic energy. The curves are calculated for three different positions (1) Br on Li^+ site and $\phi=45°$, i.e., the equilibrium position (solid curve); (2) Br on Li^+ site and $\phi=0°$ (dashed curve); (3) Br on saddle point site and $\phi=0°$ (dotted curve).

0.04 eV at a substrate temperature of 10 K due to improved localization of the scattering. Once again the H-beam E'_{TRANS} will not show a comparable narrowing at lower temperatures, since the beam scatters off all points of the substrate surface.

A change in the incident kinetic energy of the photofragment H-atom E'_{TRANS} will affect the adsorbed-state scattering angle distribution. The gas phase photolysis of a HBr molecule by 248 nm laser radiation will yield a H-atom with a kinetic energy of ~ 1.1 eV in contrast to the 2.6 eV employed until now. Even though in the adsorbed state H does not fully separate from Br before colliding with an adjacent F^-, the H-photofragment produced by 248 nm radiation will nonetheless have a lower collision energy E_{TRANS} at the turning point of its collision than did the H-photofragment produced by 193 nm radiation (see Fig. 2.). At the lower E_{TRANS} the H-photofragment will not penetrate as deeply into the impacted F^-, but will scatter off an outer potential-energy contour as indicated in the figure. A comparison of the scattering distributions for H-atoms with the nominal 2.6 as compared with 1.1 eV of kinetic energy is shown in Fig. 5. At 1.1 eV the scattering angle maximum has decreased to $\theta'=45°$. The FWHM shows little change since it depends primarily on the temperature of the substrate.

The decrease in scattering angle with decreasing E_{TRANS} is a general trend as is shown in Fig. 6 where the scattering angle as a function of kinetic energy is plotted for three combinations of sites and orientations (1) Br above the Li^+ site with the H atom tilted 26° below the surface horizontal towards a neighboring F^- ($\theta=64°$, $\phi=45°$) i.e., in the equilibrium position; (2) Br above the Li^+ site with the H tilted downwards towards a neighboring Li^+ ($\theta=64°$, $\phi=0°$); and (3) Br above the saddle point site with the H tilted downwards towards a neighboring Li^+ ($\theta=64°$, $\phi=0°$). For all three cases the scattering is closest to specular ($\theta'=\theta$) at high energy. The greatest deviation, $\theta'\neq\theta$, is for $\phi=45°$ for which the Li^+ and F^- alternate. Less corrugation for $\phi=0°$ (top two curves of Fig. 6) evidences itself as less deviation of θ' from θ.

An examination of the scattering angle, θ', as a function of incident angle, θ, is shown in Fig. 7 for the same three site-orientation combinations considered in the previous figure. All of the curves show a linear relationship between θ' and θ with the 45° azimuthal orientation showing the greatest nonspecularity, $\theta'<\theta$, in keeping with maximum surface corrugation along that azimuth. This linear relationship indicates that the form of the incident angle distribution will be preserved during the scattering process and thus can lead to surface-aligned inelastic events, such as surface aligned photoreaction.

Finally, in Fig. 8 we compare the computed scattering angle distributions for the PDIS of HBr/LiF(001) at 100 K with the experimental results of Bourdon *et al.*[7] In addition we also show in Fig. 8 preliminary calculations done at a coverage of 0.2 ML where the H-photofragment is allowed to interact with coadsorbed HBr molecules. These

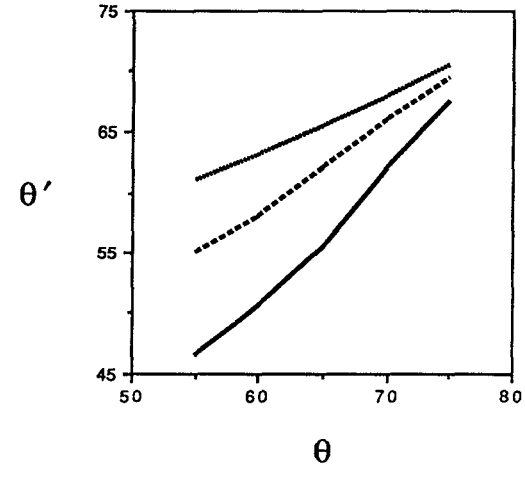

FIG. 7. Scattering angle θ' as a function of incident angle θ for the three cases considered in Fig. 6.

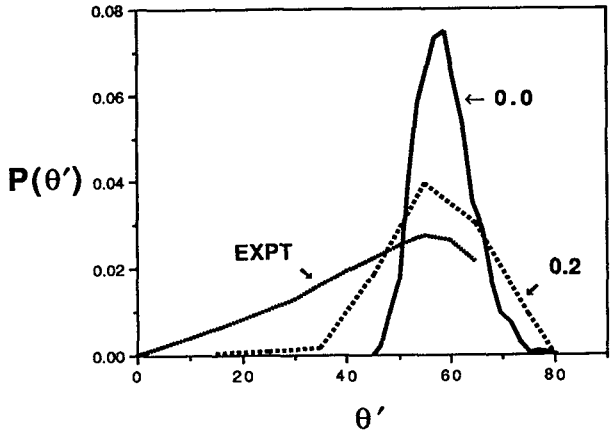

FIG. 8. Comparison of the calculated (0.0 and 0.2 ML shown as the solid and dashed curves, respectively) and experimental (0.2 ML shown as the dotted curve) scattering angle distributions at 100 K.

higher coverage results will be reported *in extenso* in a later paper.[12] In all cases the peak of the distributions occurred in the region 55°–60°. The calculations showed that as the coverage increased the distribution spread out and became asymmetric, biased toward smaller angles in qualitative agreement with experiment. The experimental distribution over θ' at 0.2 ML is broader than the computed one. The experimental results[7] have been multiplied by $\sin(\theta')$ in order to compare them with the azimuthally integrated results of the present calculations which give greater weight to higher θ'.

IV. CONCLUSIONS

We have examined the photodissociation of HBr adsorbed on LiF(001) and the subsequent scattering of the H-atom photofragment off the LiF surface using a stochastic classical trajectory technique. One of the motivations for the study was to determine whether the conditions needed for surface-aligned photoreaction are destroyed when one of the reagents scatters off a rough substrate prior to entering into a reactive encounter with a coadsorbed collision partner. A further motivation was to investigate "localized scattering" characteristic of adsorbate photodissociation in contrast to molecular beam scattering; the former should constitute a site-specific probe of the surface.

We have found that the H-atom photofragment scatters off the LiF surface in a nonspecular fashion, in contrast to a beam of H-atoms originating in the gas phase, by colliding exclusively with a neighboring F^- ion at the surface. Angular distributions can be made narrow by going to low substrate temperatures. The surface collision preserves the narrow incident angle distribution and transforms it into an equally narrow scattering angle distribution. It follows that control over angle of approach and impact parameter in inelastic encounters is possible even if there is surface scattering prior to the inelastic event. The nonspecularity of the scattering is a measure of the collision diameter of a specific atom, F^-. We have simulated molecular beam scattering and have found that, being nonsite-specific it peaks at the specular angle.

For photodissociation of HBr(ad) on LiF(001) with 193 nm radiation the peak of the scattering angle distribution was found to be 55°, in agreement with the experimental results ($55 \pm 5°$). This peak is predicted to shift to lower scattering angles, θ', with smaller photon energies as scattering takes place from successively lower potential energy contours (an experiment which has not yet been done, but should be). Since the photofragment strikes the surface atom in a localized area, observation of θ' as a function of photolytic wavelength should permit mapping of the potential energy contours around a specified surface atom.

ACKNOWLEDGMENTS

We thank S. O'Shea and R. Williams for their advice on interaction potentials and P. Charters for his assistance in drawing the figures. This work has been made possible through the generous assistance of the Natural Sciences and Engineering Research Council (NSERC) of Canada, Cray Research (Canada) Inc., the Ontario Center for Large Scale Computation, and the Ontario Laser and Lightwave Research Center. One of us (V. J. B.) has been supported through a NSERC postdoctoral fellowship.

[1] (a) E. B. D. Bourdon, P. Das, I. Harrison, J. C. Polanyi, J. Segner, C. D. Stanners, R. J. Williams, and P. A. Young, Faraday Discuss. Chem. Soc. **82**, 343 (1986).
[2] J. C. Polanyi and H. Rieley, in *Dynamics of Gas-Surface Interactions*, edited by C. T. Rettner and M. N. R. Ashfold (Royal Society of Chemistry, London, 1991), Chap. 8.
[3] I. Harrison, J. C. Polanyi, and P. A. Young, J. Chem. Phys. **89**, 1475 (1988).
[4] H. Guo and G. C. Schatz, J. Chem. Phys. **94**, 379 (1991).
[5] J. M. Watson, I. Noorbatcha, and R. R. Lucchese, J. Chem. Phys. **96**, 7771 (1992).
[6] M. I. McCarthy and R. B. Gerber, J. Chem. Phys. **93**, 887 (1990).
[7] E. B. D. Bourdon, C.-C. Cho, P. Das, J. C. Polanyi, C. D. Stanners, and G.-Q. Xu, J. Chem. Phys. **95**, 1361 (1991).
[8] P. M. Blass, R. C. Jackson, J. C. Polanyi, and H. Weiss, J. Chem. Phys. **94**, 7003 (1991).
[9] J. C. Polanyi, R. J. Williams, and S. F. O'Shea, J. Chem. Phys. **94**, 978 (1991).
[10] J. C. Polanyi and R. J. Williams, J. Chem. Phys. **88**, 3363 (1988).
[11] J. C. Tully, G. H. Gilmer, and M. Shugard, J. Chem. Phys. **71**, 1630 (1979).
[12] V. J. Barclay, D. B. Jack, J. C. Polanyi, and Y. Zeiri (to be published).
[13] D. Kosloff and R. Kosloff, J. Comput. Phys. **52**, 35 (1983); R. B. Gerber, R. Kosloff, and M. Berman, Comput. Phys. Rep. **5**, 60 (1986).
[14] V. J. Barclay, J. C. Polanyi, Y. Zeiri, and R. Kosloff (to be published).
[15] J. E. Lennard-Jones and B. M. Dent, Trans. Faraday Soc. **24**, 92 (1928).
[16] K. T. Tang and J. P. Toennies, J. Chem. Phys. **80**, 3726 (1984).
[17] (a) T. L. Gilbert, J. Chem. Phys. **49**, 2640 (1968); (b) T. L. Gilbert, O. C. Simpson, and M. A. Williamson, *ibid.* **63**, 4061 (1975).
[18] F. T. Smith, Phys. Rev. A **5**, 1708 (1972).
[19] H. J. Boehm and R. Ahlrichs, J. Chem. Phys. **77**, 2028 (1982).
[20] H. C. Lee and Y. S. Kim, J. Chem. Phys. **74**, 6144 (1981).
[21] P. W. Fowler and P. A. Madden, Phys. Rev. B **29**, 1035 (1984).
[22] P. W. Fowler and J. M. Hutson, Phys. Rev. B **33**, 3724 (1986).
[23] P. W. Fowler and J. M. Hutson, Surf. Sci. **173**, 337 (1986).
[24] K. T. Tang and J. P. Toennies, Z. Phys. **1**, 91 (1986).
[25] H. J. Boehm, R. Ahlrichs, P. Scharf, and H. Schiffer, J. Chem. Phys. **81**, 1389 (1984).
[26] J. D. Bowman, J. O. Hirschfelder, and A. C. Wahl, J. Chem. Phys. **53**, 2743 (1970).
[27] The parameter β is the same as the value given in Ref. 23 for the Kr–Kr

system. However, the value of the repulsion strength, A, has been used as a free parameter which has been fit to the experimental value (see Ref. 7) of the energy of adsorption.
[28] H. Chow and E. D. Thompson, Surf. Sci. **82**, 1 (1979).
[29] W. A. Steele, *The Interaction of Gases with Solid Surfaces* (Pergamon, Oxford, 1974).
[30] M. I. McCarthy, R. B. Gerber, and M. Shapiro, J. Chem. Phys. **92**, 7708 (1990).
[31] S. A. Adelman and J. D. Doll, J. Chem. Phys. **64**, 2375 (1976).
[32] M. Tosi, Solid State Phys. **16**, 1 (1964).
[33] E. Sandor and M. W. Johnson, Nature **217**, 541 (1968).